

NUMERICAL AND EXPERIMENTAL ANALYSIS OF AIR TO WATER HEAT PUMPS

Carles Oliet, Ph.D. (Mech. Eng.), Heat and Mass Transfer Technological Center (CTTC), Universitat Politècnica de Catalunya - BarcelonaTech (UPC). ETSEIAT, Colom 11, 08222, Terrassa, Barcelona, Spain.

Alexandre Sadurní, Ph.D. (Mech. Eng.), Heat and Mass Transfer Technological Center (CTTC), Universitat Politècnica de Catalunya - BarcelonaTech (UPC). ETSEIAT, Colom 11, 08222, Terrassa, Barcelona, Spain.

Nicolás Ablanque, Ph.D. (Mech. Eng.), Heat and Mass Transfer Technological Center (CTTC), Universitat Politècnica de Catalunya - BarcelonaTech (UPC). ETSEIAT, Colom 11, 08222, Terrassa, Barcelona, Spain.

Joaquim Rigola, Ph.D. (Mech. Eng.), Heat and Mass Transfer Technological Center (CTTC), Universitat Politècnica de Catalunya - BarcelonaTech (UPC). ETSEIAT, Colom 11, 08222, Terrassa, Barcelona, Spain.

Abstract: In the present work a numerical and experimental analysis of a R134a air to water heat pump is carried out. A numerical model has been developed and implemented to predict the heat pump thermal and fluid-dynamic behavior. The model is based on an object-oriented simulation tool called NEST where the whole system is modeled as a collection of different blocks linked between them. Each block represents a specific element of the system such as heat exchangers, compressors or expansion devices. The resolution procedure consists in solving all the blocks/elements iteratively until a converged solution is reached. In addition, a fully instrumented experimental facility has been built and commissioned in order to acquire experimental data and compare them against the numerical model predictions. In this work, the main aspects of the numerical model are presented together with a brief description of the experimental unit. The numerical results are compared against the experimental data and different numerical parametric studies are carried out.

Key Words: air to water heat pump, water heater, numerical model, experimental unit

1 INTRODUCTION

An air to water heat pump is a system that transfers heat from the surrounding air to stored or flowing water (the heated water may be used for different applications such as direct supply or heating purposes). Although they use energy to operate a compressor as they work under vapor compression principles, they are more efficient than conventional electric water heaters (Neksa et al., 1998). Several numerical models and experimental investigations on air to water heat pumps are published in the open literature (e.g. Fu et al. 2003, Mei et al. 2003, Kim et al. 2004, and Zhang et al. 2009). The aforementioned models are mainly oriented to solve vapor compression cycle layouts, with a certain level of flexibility, both for stationary or dynamic situations. The model proposed in this paper has a great flexibility in terms of cycle layout and components modeling level. It also has the capability to interact the heat pump model with other systems (thermal storage systems, water circuits, refrigerated chambers, buildings, etc.), even at CFD&HT level, in a single simulation platform.

The aim of this work is to develop computational tools and experimental facilities to study air to water heat pump systems. On the one hand, a flexible simulation tool to study thermal systems has been implemented. The approach of the numerical procedure presented herein is based on a modular strategy where all the system elements are considered as independent entities. The elements are linked between them so that a specific system is defined by both its elements and links. For this purpose the in-house numerical platform

called NEST is adapted to simulate air to water heat pump systems. The most significant features of the numerical infrastructure used in the global model are: i) high flexibility to include/remove elements, ii) possibility to simulate multiple related thermal systems at the same time (e.g. an air to water heat pump cycle together with the heated water loop), iii) the possibility to easily replace any numerical model of any element by a different numerical approach (e.g. a model with a high level of detail could be used in a specific element in order to investigate deeper into that element behavior), iv) easy implementation of control systems for any element or group of elements within the whole simulation system, and v) the use of system optimization techniques in order to optimize the whole system performance based on selected parameters. It is important to mention that the scope of this document is to report the first numerical results for a relatively simple heat pump system (i.e. the first step that will lead to a more comprehensive study of air to water heat pumps). On the other hand, a flexible experimental facility of an air to water heat pump, equipped with several instruments, has been developed. Experimental data has been collected at different operational conditions (condenser inlet coolant temperature ranging from 20 to 50 °C).

This document is divided in six sections. The second section is devoted to explain the modular approach while the third section presents brief descriptions of the numerical models used to simulate the system elements (e.g. heat exchangers, compressor, expansion device, etc...). In the fourth section the experimental unit is presented and relevant details are provided. All the numerical results are shown in the fifth section. A validation test is carried out along with different parametric studies to analyze the influence on the whole system of different parameters (capillary tube length, air temperature, and refrigerant mass charge). And finally, in the sixth section conclusions are given.

2 SYSTEM NUMERICAL MODEL

The numerical model is based on a modular approach where the whole heat pump vapor compression system is divided into discrete elements. Each element can be independently solved from a set of given boundary conditions. However, the whole system resolution is done iteratively by solving all its elements and transferring the appropriate information between them. The in-house object-oriented tool called NEST used for this purpose has already been applied to energy balances in buildings (Damle et al., 2011a) and hermetic reciprocating compressors (Damle et al., 2011b). The advantages of the present working methodology could be summarized as follows:

- *System layout adaptability.* The modular approach allows adding, subtracting, and substituting any element of the system. Therefore thermal systems with more/less elements are easily represented. Moreover the numerical platform allows the simultaneous simulation of any number of loops (which may be linked between them). For instance, the heat pump refrigerant loop could be solved together with the heated water loop (e.g. a secondary loop made up of a pump, a storage tank and a common heat exchanger with the main loop).
- *Replaceable element model.* Any element consists of a black box as regards the system numerical resolution procedure. Therefore, for a particular element, its model could be easily replaced by another model. For instance, the selection of the model used to simulate a heat exchanger will depend on the studied device but it may vary from a simple ϵ -NTU approach, to a distributed model considering two-phase flows or to any other model with a higher level of complexity. This feature allows to study with greater detail any specific aspect of any specific element of the cycle.
- *Compatibility with CFD analysis.* The simultaneous resolution of a whole thermal system could be directly linked with a detailed CFD analysis of any of its parts/boundaries. For instance a space cooling heat pump could be solved together with a CFD analysis of the air inside the cooled space.
- *Control capacity over system and elements.* The numerical platform allows the consideration of any type of condition over both the whole system and any of its constitutive elements. Therefore any type of control could be easily implemented

(e.g. the compressor working frequency could be regulated according to the temperature reported in the refrigerated chamber during a transient simulation).

- *System optimization techniques.* The whole system resolution could be also coupled with a numerical algorithm used to find optimal operational or geometric conditions of any of its constitutive parts. For instance, a genetic algorithm is being currently implemented.

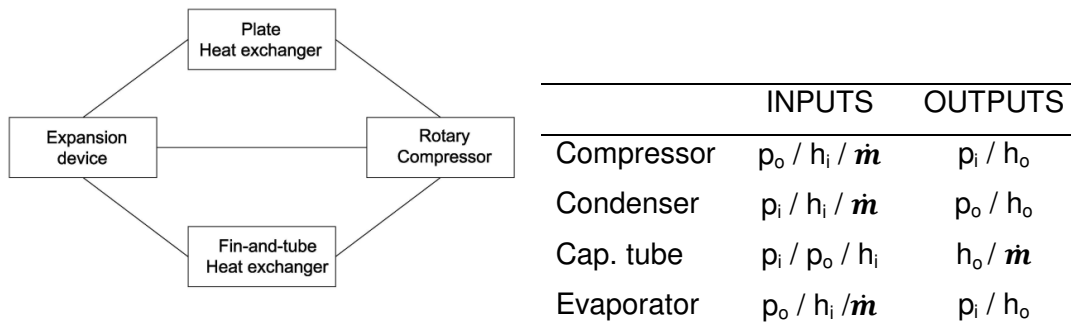


Figure 1: Block diagram (left) and element transfer data scheme (right)

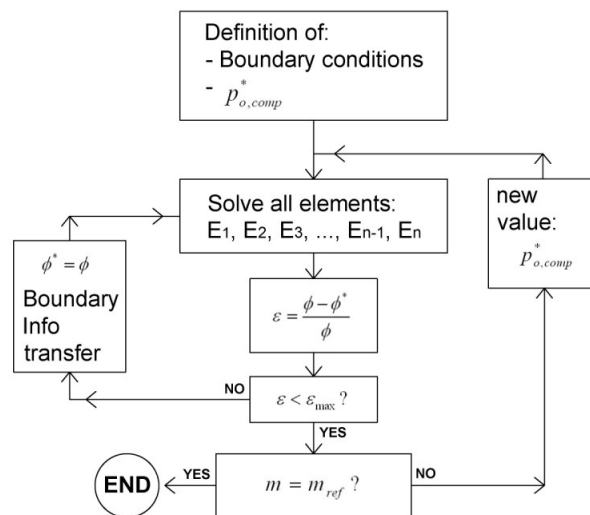


Figure 2: Resolution scheme for steady-state heat pump

In this work the modular approach is applied to steady-state air to water heat pumps. In Figure 1 the simplified block diagram of a heat pump system is presented together with the elements transfer data scheme (all minor elements are neglected for clarity purposes). The refrigerant enthalpies and pressures defined at the elements boundaries together with a common mass flow rate - shared by all the elements - constitute the system variables. It can be noticed that the resulting set of equations is indeterminate and therefore one of the system variables is kept constant during the resolution process (i.e. the compressor outlet pressure). In order to overcome this limitation, and to achieve full closure, the refrigerant mass inside the whole system must be known and a new iterative loop must be added (see Figure 2). In this way, after each system converged solution for a specific compressor outlet pressure, the current system mass is calculated (by adding up the refrigerant mass inside each element) and compared against the defined mass for the system. If the calculated mass does not match with the reference mass a new iteration starts with a corrected compressor outlet pressure.

3 COMPONENT NUMERICAL MODELS

The studied heat pump system is basically made up of the following elements: a rotary compressor, a plate heat exchanger condenser used to heat up water of an auxiliary circuit, a fin-and-tube heat exchanger evaporator used to extract heat from the surrounding air, a capillary tube used as the expansion device, and finally different connecting tubes and other additional elements (oil separator, valves, etc...). The simulation approaches used to predict the thermal and fluid-dynamic behavior of the most relevant elements are explained in the following sections.

3.1 Compressor

A simplified approach is used to simulate the rotary compressor and calculate three essential parameters: the energy consumption, the mass flow rate, and the fluid enthalpy leap between the compressor inlet and outlet positions.

First, the mass flow rate is calculated from the volumetric efficiency which is defined as the ratio between the current mass flow rate and the ideal mass flow rate: $\eta_v = \dot{m} / (\rho_i N V_{cl})$. This efficiency can be also expressed as a function of the compression ratio when constant rotation speed is considered (Wenhua Li, 2013). Therefore, a relationship between the volumetric efficiency and the compression ratio for the commercial compressor studied herein has been empirically obtained. Second, the heat gained by the fluid is deduced from a global heat balance over the compressor based on a constant mechanical-electrical efficiency which is also empirically adjusted. It is important to notice that the experimental dataset used for this purpose was independent from that used for the model validation (see Section 5.1). And third, the compressor energy consumption is directly calculated from the system pressures (evaporating and condensing) and a curve provided by the manufacturer.

3.2 Heat exchangers

For both plate and fin-and-tube heat exchangers different levels of simulation could be considered. First, the detailed model called CHESS (Oliet *et al.* 2002) where the domain is divided into a set of control volumes (e.g. fin-and-tube blocks for the fin-and-tube heat exchanger). The model allows steady and unsteady analysis, flexible geometry and circuitry, working at dry or wet/frosting conditions. The inner refrigerant flow is solved with a two-phase flow model where non-uniform heat transfer coefficients can be considered in radial and axial directions (Oliet *et al.* 2010). Second, a numerical model based on a lumped approach (Oliet *et al.* 2007). In this case the heat exchanger is divided into different macro zones where semi-analytic methods (ϵ -NTU and $F\text{-}\Delta T_{lm}$) are applied. The condenser is divided in three different zones (super-heated gas, two-phase, and sub-cooled liquid) as well as the evaporator (two-phase flow, dry-out, and super-heated gas). Each of the defined zones has different phenomenological characteristics and considerations. The second method considers a uniform behavior within each zone (i.e. constant physical properties and constant heat transfer coefficient), although the size of each zone is iteratively calculated by a combination of rating and design ϵ -NTU calculations. In fact, its multi-zonal nature allows the model to adapt fairly well to heat exchanger sections having different global heat transfer coefficients. All the geometrical details and specific zone-based correlations are considered in this model. The lumped model has been extensively validated in previous works. It has been chosen for the present work because of its fast response and its reasonable good accuracy which are appropriate for the simulation of a whole system (e.g. heat pump water heaters). For more detailed studies with the focus shifted to the detailed analysis of the heat exchangers or the transient response of the heat pump, the detailed model would be considered.

3.3 Expansion device

The algorithm to simulate the capillary tube is based on a two-phase flow distributed model presented by García-Valladares *et al.* (2004). The fluid domain is represented by means of

consecutive control volumes where the governing equations (continuity, momentum and energy) are applied and solved:

$$\frac{d\bar{m}}{dt} + \dot{m}_i = \dot{m}_{i-1} \quad (1)$$

$$\frac{d\bar{m}\bar{v}}{dt} + \dot{m}_{g,i}v_{g,i} + \dot{m}_{l,i}v_{l,i} - \dot{m}_{g,i-1}v_{g,i-1} - \dot{m}_{l,i-1}v_{l,i-1} = (p_{i-1} - p_i)S - \bar{\tau}\pi D\Delta z_i - mgsin\theta \quad (2)$$

$$\frac{d\bar{m}(h + \bar{e}_c + \bar{e}_p)}{dt} + \dot{m}_i(h + e_c + e_p)_i - \dot{m}_{i-1}(h + e_c + e_p)_{i-1} = \dot{Q}_{wall} + V\frac{dp}{dt} \quad (3)$$

The flow is evaluated on the basis of a step-by-step numerical implicit scheme where the wall temperature map acts as the boundary condition. The formulation requires the use of empirical correlations to evaluate the void fraction (ϵ), the shear stress ($\bar{\tau}$) and the convective heat transfer coefficient used to evaluate the heat transferred between the tube and the fluid (\dot{Q}_{wall}).

The capillary tube resolution procedure is carried out in two steps. The first step consists in determining if the capillary tube is working at critical or non-critical conditions, while the second consists in performing the simulation according to the condition. More details of this model are found in Ablanque *et al.* (2010).

Critical condition determination. The mass flow rate inside a capillary tube increases as the evaporating temperature decreases (lower discharge pressure) but only up to a critical value from which the mass flow rate remains constant. This critical limit occurs when the entropy generation equation is not anymore accomplished ($s_{gen,i} < 0$):

$$\dot{m}_{i-1}s_{i-1} + \dot{m}_i s_i - \frac{\bar{q}_i}{T_{wall}}\pi D\Delta z_i = \dot{s}_{gen,i} \quad (4)$$

Alternatively this limit can be calculated when dp/dz approaches to infinity (or $dz/dp < \epsilon$). Therefore, when the latter equation is not accomplished at the capillary tube outlet end (last control volume) critical conditions are met (i.e. critical mass flow rate and discharge pressure). It is convenient to use a non-uniform grid for the fluid domain discretization due to the high pressure gradients.

Critical and non-critical flow resolution. The flow is critical when the critical discharge pressure is higher than the actual discharge pressure and non-critical in the opposite case. If the flow is non-critical new iterations are carried out in order to find the refrigerant thermal and fluid-dynamic behaviour taking into account the actual discharge pressure. However, if the flow is critical, an additional control volume is considered at the capillary tube outlet end. There, an energy balance is applied to calculate the capillary tube discharge enthalpy (heat transfer and transient terms are neglected).

3.4 Additional elements

Additional elements have been taken into account for the simulations carried out in this work. For instance, to simulate the connecting tubes between the main elements, the flow model presented in Section 3.3 has been used. Other minor elements, such as the mass flow meter, have been simulated in order to predict their pressure losses.

4 EXPERIMENTAL SET-UP

A highly instrumented experimental facility has been constructed to study the performance of air to water heat pumps and to provide useful data to test numerical codes. A schematic overview of the experimental unit is depicted in Figure 3. The current experimental set-up will be used as the foundational platform for further experimental studies and tests with different refrigeration fluids and cycle components.

The unit main loop works with R134a and includes the following elements: a rotary compressor, an oil separator, a plate heat exchanger (condenser), a capillary tube as the expansion device and a fin-and-tube heat exchanger (evaporator). Several measuring instruments are placed throughout the main loop path: type K thermocouples and/or thermoresistances to measure the refrigerant inlet and outlet temperatures of each element, a Coriolis mass flow meter located after the oil separator, two pressure transducers and two differential pressure sensors to measure the absolute high and low system pressures and the most relevant pressure drops.

The condenser secondary circuit works with a water/glycol mixture and includes the following elements: a thermostatic bath to control the coolant temperature and a pump to drive the fluid. It also includes both type K thermocouples and Pt-100 thermoresistances at the inlet and outlet positions of the condenser, and a Coriolis mass flow meter located before the thermostatic bath.

The evaporator external fluid is air driven by a fan. The air channel is equipped with a turbine speed sensor together with capacitive sensors of both temperature and relative humidity located at both the entrance and the exit of the evaporator.

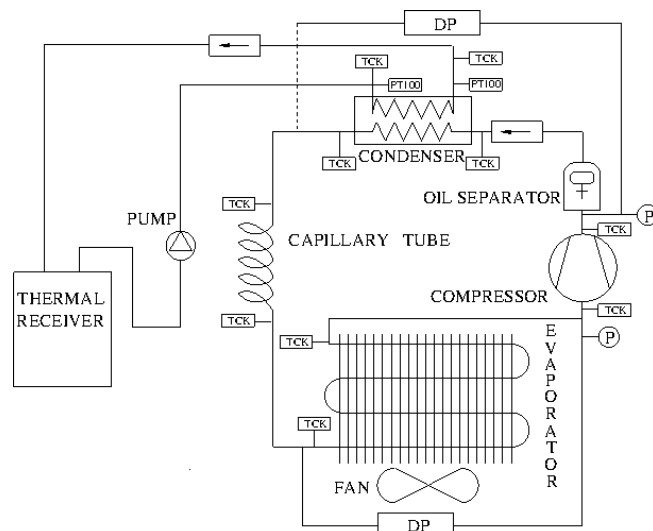


Figure 3: Simplified scheme of the experimental facility

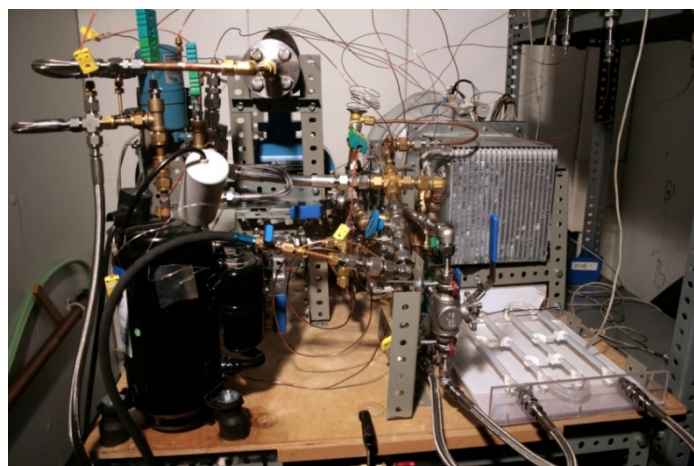


Figure 4: Experimental facility photograph

All the components of the whole facility – including the connection pipes but not the compressor – are covered with an insulation layer to prevent heat losses. The main details of the elements are described as follows:

- Compressor: Rotary R134a; N = 50 Hz; $V_{cl} = 18 \text{ cm}^3$

- Condenser: Plate heat exchanger
- Capillary tube: L = 1.5 m; D = 1.5 mm
- Evaporator: Fin-and-tube heat exchanger

4.1 Experimental tests

A set of steady-state experimental tests has been carried out considering different working conditions varying the condenser secondary loop inlet temperature. The testing conditions are detailed in the following list:

- Evaporator air inlet temperature: 20 °C
- Evaporator air mass flow rate: 450 kg/h
- Evaporator air relative humidity: 28 %
- Condenser coolant inlet temp: 20/30/40/50°C
- Condenser coolant flow rate: 280 kg/h

For each run, the steady-state regime was achieved when all the system parameters remained constant. The coolant (water + propylene glycol 40%vol.) temperature was controlled by means of the thermostatic bath. The system refrigerant mass remains constant for all the cases.

5 NUMERICAL RESULTS

5.1 Comparison vs. experimental data

In this section the numerical results obtained with the numerical model presented in Sections 2 and 3 are compared against the experimental data acquired in the experimental unit described in Section 4. The results are plotted in Figure 5 where relevant cycle parameters are shown for the whole range of the condenser auxiliary circuit inlet temperature. It is noticed that two system high pressures are reported due to the considerable pressure drop observed along the connecting tube between the compressor and the condenser inlet (presence of oil separator and flow-meter). The higher pressure corresponds to the compressor outlet while the other stands for the condensing pressure.

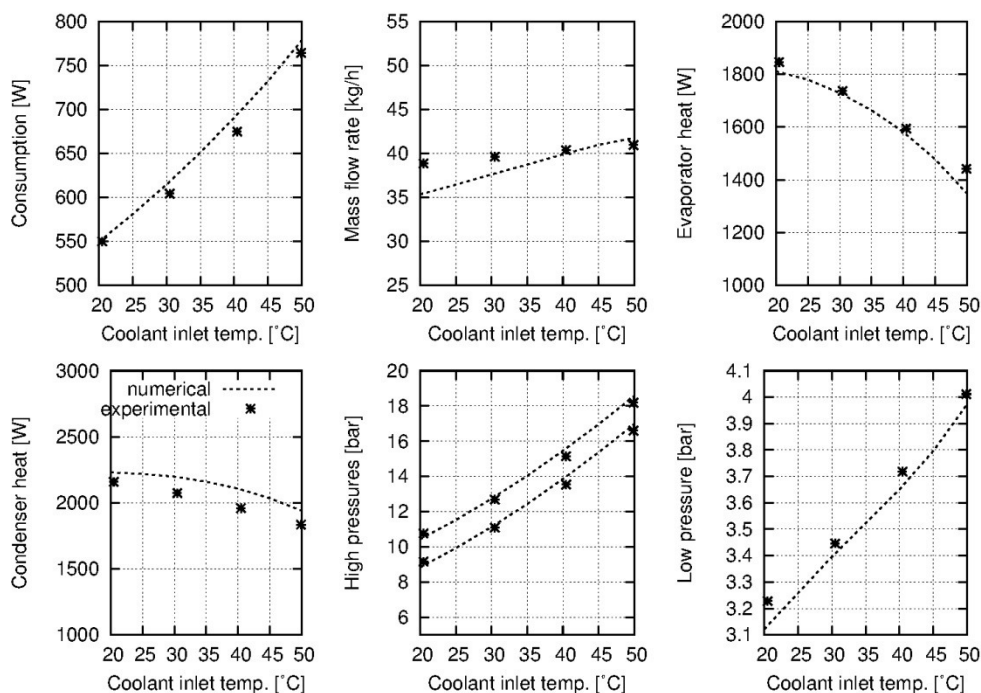


Figure 5: Numerical results vs. experimental data (coolant temperature from 20 to 50 °C)

From Figure 5 it is observed how, as the condenser water/glycol mixture inlet temperature increases, the system condensing pressure rises in order to have a sufficiently large

temperature gradient so that the refrigerant could condensate. This process is adjusted by the capillary tube behavior: an incomplete condensation process would result in a poor performance of the capillary tube, leading to a mass flow rate reduction, which in turn, leads to a better condensation process. As a result, the greater condensing pressure together with the slightly larger evaporating pressure produces a higher compressor energy need.

In the same way, the system capacity to transfer heat from the heat source to the heat sink is reduced as the heat sink temperature rises. This characteristic is well observed from both the evaporator and the condenser heat evolution graphics (both present similar decreasing trends).

The numerical results present very similar trends to the experimental observations so that good qualitative agreement is achieved. The quantitative discrepancies are reasonable good as all the numerical data falls within $\pm 10\%$ of the experimental data.

4.2 Parametric studies

In this Section the influence of three different system characteristics is studied: the capillary tube total length, the evaporator secondary circuit air inlet temperature, and the system total refrigerant mass flowing through the main loop. The reference case conditions for this parametric study are resumed in Table 1.

Table 1: Numerical conditions for parametric studies

Capillary tube length [m]	1.5/ 2.0 */2.5/3.0
Evaporator air inlet temp. [°C]	17/19/ 21 /23/25
System refrigerant mass X [kg]	-10%/-5%/+ 0 %/+5%/+10%

* reference case in bold

Capillary tube total length. Figure 6 shows the influence of the capillary tube length over the whole cycle. As the capillary tube length increases the resistance to flow also increases at each fixed condenser secondary circuit inlet temperature. The system compression ratio is significantly greater as the high pressure rises while the low pressure diminishes. The resulting mass flow rate is lower leading to a poorer cycle performance with lowered capacity and incremented energy consumption (COP deterioration).

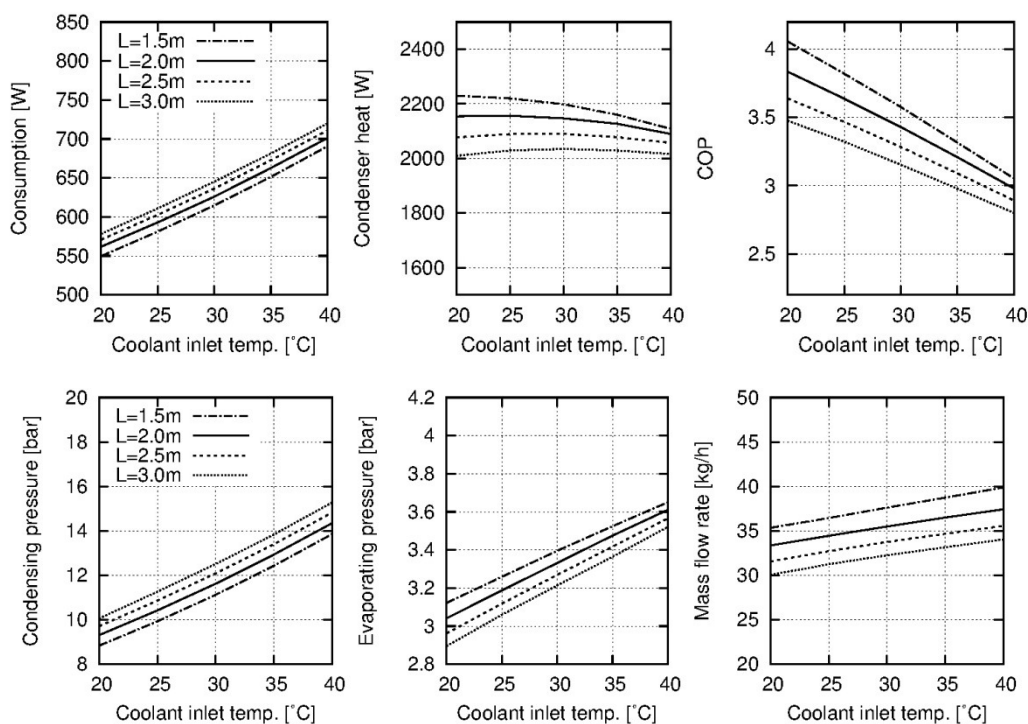


Figure 6: Numerical results: influence of capillary tube length

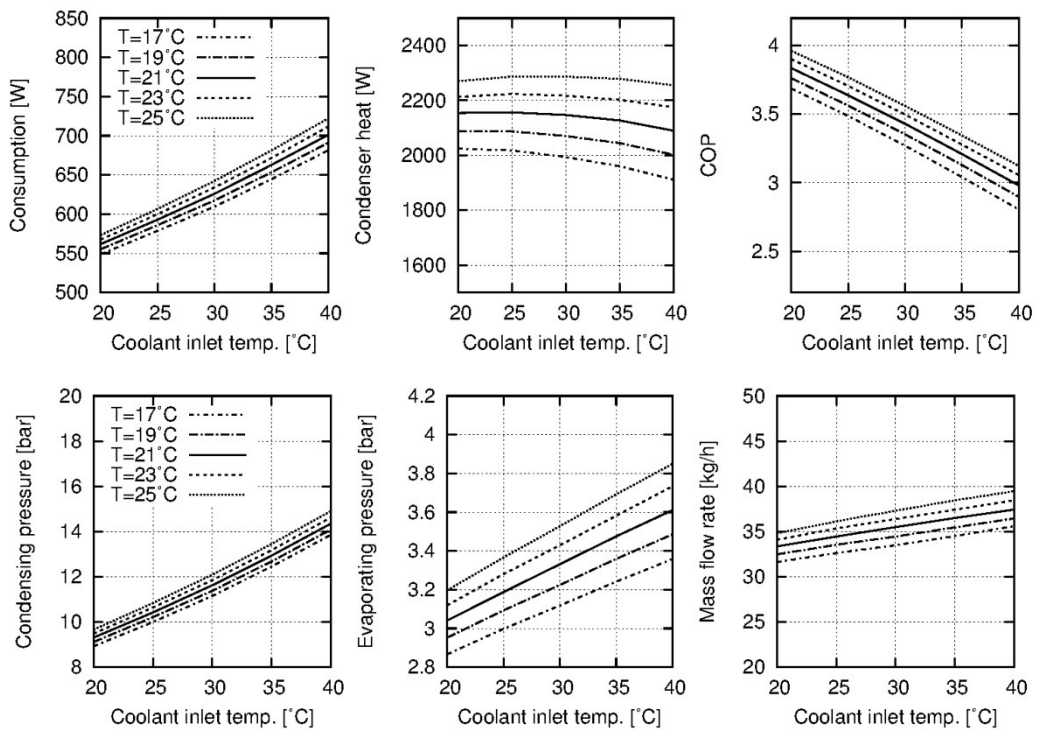


Figure 7: Numerical results: influence of external air temperature

Air inlet temperature. The influence of the air inlet temperature is studied in Figure 7. It is observed that the evaporator external air temperature rise allows the system evaporating pressure to increase together with the condensing pressure. This change combined with a higher mass flow rate results in a much better condenser heat transfer. In addition, The COP is enhanced as the energy consumption increase is, comparatively, less significant.

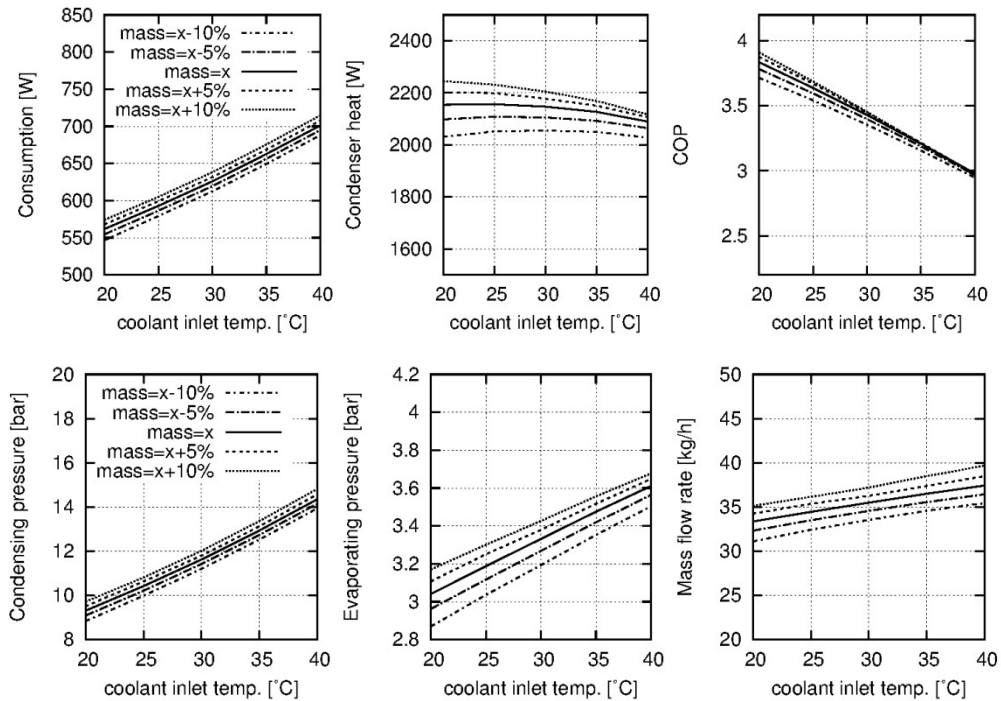


Figure 8: Numerical results: influence of system mass charge

System refrigerant mass. Figure 8 shows the evolution of the main system parameters as the system charge is modified. This unit does not include a liquid receiver - where the refrigerant mass could accumulate - and therefore the system mass is distributed among the main system elements for each numerical simulation. As the system mass rises, the mass flow rate becomes higher, both the condensing and the evaporating pressures increase, as well as the resulting energy consumption.

6 CONCLUSIONS

This work represents a first step for studying air to water heat pumps. The numerical and experimental foundations for an upcoming extensive study on heat pumps have been established.

The numerical model based on the modular approach has been successfully implemented. A reasonable agreement has been obtained between the simulations and the experimental data. The numerical platform allows an easy addition, subtraction or substitution of any element of the system. This feature gives great flexibility to the model, not only because the configuration of the system can be clearly altered, but also because the numerical model of any element can be easily replaced allowing different levels of simulation. More comprehensive analyzes of air to water heat pumps, considering a wide variety of geometrical modifications and operational conditions, are now possible. More specifically, the subsequent research step to be done consists in simulating a combined system (heat pump refrigeration cycle and heated water loop/thermal storage tank), including a control protocol, and to couple it with a genetic algorithm in order to carry out an optimization study.

An experimental unit has been developed and tested for the first time. The collected data was useful to show the system response at different coolant temperatures and to validate the numerical code. The experimental unit includes other elements that were not mentioned in this work (e.g. a thermostatic valve placed in parallel with the capillary tube). In fact, the current experimental set-up will be used as the foundational platform for further experimental studies and tests with different refrigeration fluids and cycle components.

7 NOMENCLATURE

D	diameter	(m)	Superscripts		
e	specific energy	(J kg ⁻¹)	o	previous instant	
g	gravity acceleration	(ms ⁻²)	*	guessed value	
h	specific enthalpy	(J kg ⁻¹)	Subscripts		
m	mass	(kg)	c	cylinder/kinetic	
\dot{m}	mass flow rate	(kg s ⁻¹)	g	gas phase	
N	frequency	(Hz)	i	inlet, grid position	
p	pressure	(Pa)	l	liquid phase	
\dot{Q}	heat	(W)	o	outlet	
\dot{q}	heat flux	(Wm ⁻²)	p	potential	
S	cross section	(m ²)	ref	reference	
s	specific entropy	(J kg ⁻¹ K ⁻¹)	Greek		
\dot{s}_{gen}	generation of entropy	(J K ⁻¹ m ⁻³ s ⁻¹)	ε	Conv. criteria	(-)
T	temperature	(K)	η	efficiency	
t	time	(s)	θ	inclination angle	(rad)
V	volume	(m ³)	ρ	density	(kg m ⁻³)
v	velocity	(m s ⁻¹)	τ	shear stress	(Pa)
z	axial position	(m)	φ	variable	(-)

8 REFERENCES

Ablanque N., Rigola J., Pérez-Segarra C.D., Oliva A.(2010)“Numerical simulation of capillary tubes. Application to domestic refrigeration with isobutane”*Proceedings of the 13th Int. Ref. and Air Conditioning Conference at Purdue*. West Lafayette.

- Damle R., Lehmkuhl O., Colomer G., Rodríguez I.(2011a)"Energy simulation of buildings with a modular object oriented tool" *Proceedings of the ISES Solar World Congress*, Kassel, Germany, p. 1-11.
- Damle R., Rigola J., Pérez-Segarra C.D., Castro J., Oliva A.(2011b)"Object oriented simulation of reciprocating compressors: Numerical verification and experimental comparison." *International Journal of Refrigeration* 34 (8), p. 1989-1998.
- Fu L., Ding G., Zhang C. (2003) "Dynamic simulation of air-to-water dual mode heat pump with screw compressor" *Applied Thermal Engineering* 23, p. 1629-1645.
- García-Valladares O., Pérez-Segarra C.D., Rigola J. (2004) "Numerical simulation of double- pipe condensers and evaporators" *International Journal of Refrigeration* 27 (6), p. 656-670.
- Zhang J., Wang R.Z., Wu J.Y. (2007) "System optimization and experimental research on air source heat pump water heater" *Applied Thermal Engineering* 27, p. 1029-1035.
- Kim M., Kim M.S., Chung J.D. (2004) "Transient thermal behavior of a water heater system driven by a heat pump" *International Journal of Refrigeration* 27, p. 415-421.
- Mei V.C., Chen F.C., Domitrovic R.E., Kilpatrick J.K, Carter J.A. (2003) "A study of a natural convection immersed condenser heat pump water heater" *ASHRAE trans* 109 part 2.
- Morales-Ruiz S., Rigola J., Pérez-Segarra C.D., García-Valladares O. (2009) "Numerical analysis of two-phase flow in condensers and evaporators with special emphasis on single-phase/two-phase transition zones" *Applied Thermal Engineering* 29 (5-6), p. 1032-1042.
- Neksa P., Rekstad H., Zakeri R., Schiefloe P.A. (1998) "CO₂-heat pump water heater: characteristics, system design and experimental results" *International Journal of Refrigeration* 21 (3), p. 172-179.
- Oliet C., Pérez-Segarra C.D., Castro J., Oliva A. (2010) "Modelling of fin-and-tube evaporators considering non-uniform in-tube heat transfer" *International Journal of Thermal Sciences* 49 (4), p. 692-701.
- Oliet C., Pérez-Segarra C.D., Danov S., Oliva A. (2007) "Numerical simulation of dehumidifying fin-and-tube heat exchangers: Semi-analytical modeling and experimental comparisons" *Int. J. Refrigeration* 30, p. 1266-1277.
- Oliet C., Pérez-Segarra C.D., Danov S., Oliva A. (2002) "Numerical simulation of dehumidifying fin-and-tube heat exchangers. Model strategies and experimental comparisons" *Proceedings of the Int. Refrigeration Engineering Conference*, Purdue, US
- Wenhua Li (2013) "Simplified steady-state modeling for variable speed compressor." *Applied Thermal Engineering* 50, p. 318-326.

9 ACKNOWLEDGEMENT

This work has been developed within the research project "Numerical simulation and experimental validation of liquid-vapour phase change phenomena. Application to thermal systems and equipments-II" (ENE2011-28699) of the Spanish Government.